DOI 10.1007/s11182-016-0862-0

Russian Physics Journal, Vol. 59, No. 7, November, 2016 (Russian Original No. 7, July, 2016)

STRUCTURAL STATE OF A WELD FORMED IN ALUMINUM ALLOY BY FRICTION STIR WELDING AND TREATED BY ULTRASOUND

V. A. Klimenov,[2,3] Yu. A. Abzaev,[3] A. I. Potekaev,[1,4] V. A. Vlasov,[2,3] A. A. Klopotov,[1,3] K. V. Zaitsev,[5] A. V. Chumaevskii,[3] S. A. Porobova,[3] L. S. Grinkevich,[1] I. D. Tazin,[6] and D. I. Tazin[6]

UDC 669.24' 783:539.389.1

The experimental data on structural state of an aluminum alloy, AlMg6*, in the weld zone formed by friction stir welding are analyzed in order to evaluate the effect of its subsequent ultrasonic treatment. It is found that the crystal lattice transits into a low-stability state as a result of combined heat-induced and severe shear deformation. This transition is accompanied by considerable structural-phase changes that are manifested as an increased lattice parameter of the solid solution. This increase is caused by both high values of internal stresses and increased concentration of* Mg *atoms in the solid solution due to essential dissolution of the β-*Al_2Mg_3 *particles with the content of manganese higher than that in the matrix. This is accompanied by high-intensity diffusion and relaxation processes due to the low-stability state of crystal lattice (inhomogeneous stresses) in the weld zone.*

Keywords: friction stir welding, aluminum alloy, structural state, first- and second-order stresses.

INTRODUCTION

Friction stir welding (FSW) is a well-established technique for bonding metals and alloys [1, 2]. Weld strength is especially critical in the cases where the presence of residual stresses is of great concern and for the purpose of bonding difficult-to-weld materials. An extension of FSW application area requires a deeper insight into the processes taking place during consolidation of materials under conditions of large deformations and at temperatures lower than that of melting, T_{melt}, which are frequently sufficient for phase transformations to occur [2].

The method of bonding materials by high-rate rotation along the weld joint boundary is the major technique of welding AlMg6 aluminum-manganese alloys nonhardenable by heat treatment [1]. In the contact zone of the weld, local temperature gradients (0.5–0.6 T_{melt}) are developed and the welding seam is formed as a result of stirring of solid-state materials. The features of structure formation of such welds have been extensively studied, while a comparative analysis of the resulting structural states and long-range stress fields in different weld zones is still lacking. Without understanding their complex interrelations it is difficult to predict reliable performance of a weld joint. When calculating the field stresses it is important to take into consideration the temperature dependences of elastic

[1]National Research Tomsk State Unviersity, Tomsk, Russia, e-mail: nasty_saturn@mail.ru; [2]National Research Tomsk Polytechnic University, Tomsk, Russia, [3]Tomsk State Architecture and Building University, Tomsk, Russia, e-mail: nauka@tsuab.ru; Abzaev2010@Yandex.ru; vik@tsuab.ru; klopotovaa@tsuab.ru; tch7av@gmail.com; porobova.sveta@yandex.ru; [4]V. D. Kuznetsov Siberian Physical-Technical Institute at Tomsk State University, e-mail: kanc@spti.tsu.ru; [5]Yurga Technological Institute of Tomsk State Polytechnic University, Yurga, Russia, [6]Siberian State Medical University, Tomsk, Russia, e-mail: I.D.Tazin@yandex.ru; varan2012@sibmail.com. Translated from Izvestiya Vysshikh Uchebnykh Zavedenii, Fizika, No. 7, pp. 53–58, July, 2016. Original article submitted April 27, 2015; revision submitted December 23, 2015.

TABLE 1. Composition of AlMg6 Aluminum Alloy

Elements	Si	Fe	Cu	Mn	Mg	Zn	Al
Content, at.%	0.40	0.40	0.10	0.7–1.1	5.5–6.5	0.20	~92.5%

characteristics and lattice parameters [3], since the formation of laminated ultrafine-grained structure was revealed in the center of the weld joint [4]. This structural-phase state is thought to give rise to considerable internal stresses. The stressed state of weld joints is commonly controlled by their subsequent treatment. Considering the features of FSW, nonthermal treatment processes are most applicable. Ultrasonic treatment reduces the number of defects in the weld joint [5], so its application makes it possible to considerably improve surface finish, which favorably affects the weld fatigue properties.

It should be noted that at present a lot of attention is given to metal systems demonstrating low-stability states in the regions preceding phase transitions or alloys subjected to severe deformation, which contain a large number of defects [6–8]. In most cases, these states are achieved via special technical processes [8]. Note also that the physical reasons of stability, behavior, properties and structure of such materials often remain unclear. It is quite probable that friction stir welding involves a transition into low-stability states.

The purpose of this work is to identify the interrelations between the structural state of weld joints and long-range stresses using an AlMg6 aluminum alloy in the initial state and in the weld zone during friction stir welding.

MATERIAL AND EXPERIMENTAL PROCEDURE

The experiments were performed using an AlMg6 alloy as an example in its initial state and in the weld zone in the course of friction stir welding. The alloy composition is given in Table 1 (its Russian designation is 1561). The weld zone of a weld joint is formed with AlMg6 by friction welding via high-velocity rotation of the tool, the weld zone temperature being as low as ~0.6 T_{melt}.

The weld joint was formed under optimal process conditions, which ensured high strength characteristics of the joint [9] due to thermomechanical processes in the weld zone. Subsequently, the specimens under study were subjected to a finishing ultrasonic treatment.

Ultrasonic treatment consisted in the following: the surface was processed by a hard-alloy ball striking it at the frequency 24 kHz, which was simultaneously denting into the surface by a static force at a constant pressure. The energy into the treatment zone was delivered by the static force pressing the tool to the processed surface. The indenter plastically deformed the surface layer modifying the weld structure. Ultrasonic treatment is accompanied by a number of features controlled by impact loading, periodically reciprocating and propagating over a comparatively small area. The processed surface is thus subjected to frequently interchanging compressive and shear deformations. The ultrasonic treatment was performed at the power 200 W, the indenter oscillation amplitude 20 μm, and the static force 70 N.

Diffraction studies were performed in a DRON4-07 diffractometer using CuK_α-radiation within the Bragg-Brentano geometry with the step 0.02° and the exposure time in the point 1 s within the angular range $2\Theta = 17–102°$. The diffraction patterns were taken from different spots of the specimen (Fig. 1). Their qualitative phase analysis was carried out using the Match! software program. The lattice parameter of the AlMg6 solid solution was calculated by the Rietveld method, which relied on processing the diffraction data [3].

The first- and second-order stresses were estimated by the following formulas, respectively:

$$\sigma_{\text{I}} = \frac{E}{\mu}\varepsilon_{\text{disp}} = \frac{E}{\mu}\frac{\Delta g}{g} \text{ and } \sigma_{\text{II}} = \frac{E}{\mu}\varepsilon_{\text{broad}}, \quad (1)$$

where E is the Young modulus, μ is the Poisson ratio, g is the interplanar spacing for the reflection planes, $\varepsilon_{\text{disp}}$ is the deformation due to displacement of reflections, and $\varepsilon_{\text{broad}}$ is the deformation due to broadening of reflections. For cubic

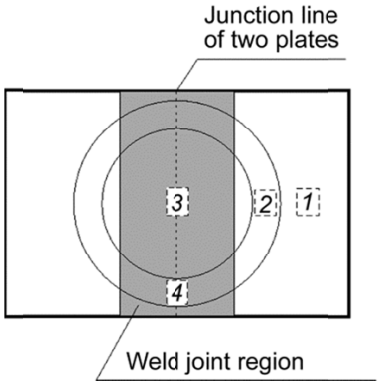

Fig. 1. Schematics of X-ray photography and microhardness measurements in different regions: *1* – initial state, *2* – far from the weld, *3* – weld joint, *4* – weld after ultrasonic treatment.

crystals $\Delta g / g = \Delta a / a$, where a is the lattice parameter. At room temperature, the Young modulus and the Poisson ratio were taken to be E = 65.79 GPa and μ = 0.337, respectively [10].

The inhomogeneous fields of internal stresses (second-order stresses) were evaluated from the reflection broadening using the Warren – Averbach analysis [3]. Note that it was taken into account that a decrease in the coherently diffracting domains (CDDs) also gives rise to broadening of the Bragg reflections from the solid solution [3].

Microhardness was measured in an MPT-3M hardness tester, with a fresh chip of a NaCl crystal serving as a test object. The indentations were formed using a diamond four-face pyramid. The load on the specimen was taken to be 10 gf. The microhardness was measured on the plate specimens of the alloy in the sites indicated in Fig. 1.

RESULTS AND DISCUSSION

Ultrasonic treatment was performed at the power 200 W, the indenter oscillation amplitude 20 μm, and the static power 70 N. The weld joint was formed by FSW under conditions of material heating via friction with a special rotating tool and stirring of the material in its plastic state under pressure. The structural and phase transformations, accompanying the process of material consolidation in the weld zone, generally ensure improved microhardness and weld joint strength [9]. It is well known that a subsequent ultrasonic treatment allows reducing roughness in the weld joint zone and, due to additional deformation of the surface layers, results in increased microhardness. These positive changes are associated not only with grain structure refinement but also with phase transformations taking place in the solid phase. These complex transformations apparently affect the first- and second-order stresses.

A qualitative phase analysis of the diffraction patterns (Fig. 2) demonstrated that the major phase is a solid solution based on the crystal lattice of aluminum (Al-base solid solution). According to the data reported in [9], the AlMg6 alloy contains an insignificant fraction of the β-Al_2Mg_3-phase particles (Fig. 3). This phase is also designated as β-$Al_{140}Mg_{89}$.

Using the diffraction analysis data (Figs. 2–4), we determined the lattice parameter of the solid solution of the alloy in different areas (Table 2). The experimental data on the lattice parameter of the initial solid solution (far from the weld without ultrasonic treatment) are somewhat lower than those of pure Al (a_{Al} = 0.40497 nm) [11]. It is well known that the alloying elements, such as Mg, Mn, Zn, Cu and Si, present in the Al-base solid solution affect the lattice parameter in a different manner (Fig. 5). It is evident that Mg considerably increases the lattice parameter of the solid solution, while alloying by Mn, Zn, Cu and Si reduces its values. Assuming additivity of the alloying element contributions into the lattice parameter changes, we estimated the concentration of Mg in the Al-base solid solution (Table 2). This concentration, according to the solvus curve (Fig. 6), corresponds to the heat treatment of the alloy within the temperature range 150–200°C.

TABLE 2. Structural and Mechanical Characteristics of the Al-Base Solid Solution in the Parent Phase (spatial group $Fm\bar{3}m$) in the AlMg6 Alloy

Number of area in Fig. 1	Exposure region	a, nm	σ_I, MPa	at.% Mg	HV
1	Initial state	$(0.40439 \pm 1)\cdot 10^{-5}$	0	2.2	94 ± 2
2	Far from the weld with ultrasound	$(0.40733 \pm 1)\cdot 10^{-5}$	1419 ± 10	8	98 ± 2
3	Weld zone without ultrasound	$(0.40745 \pm 1)\cdot 10^{-5}$	1477 ± 10	8	107 ± 2
4	Weld zone with ultrasound	$(0.40791 \pm 1)\cdot 10^{-5}$	1699 ± 10	9.7	126 ± 2

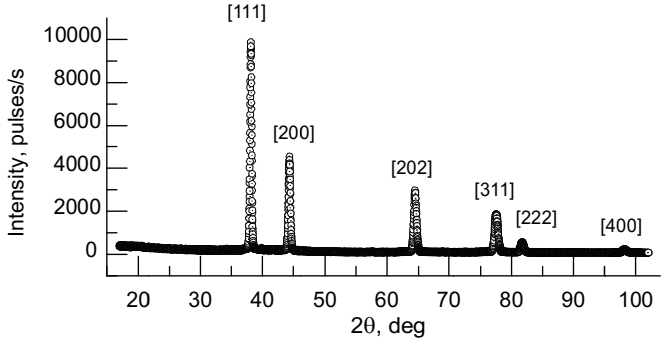

Fig. 2. Diffraction pattern from the AlMg6 alloy taken far from the weld seam zone (Area *1* in Fig. 1). The square brackets contain the indices of structure reflections from FCC-aluminum.

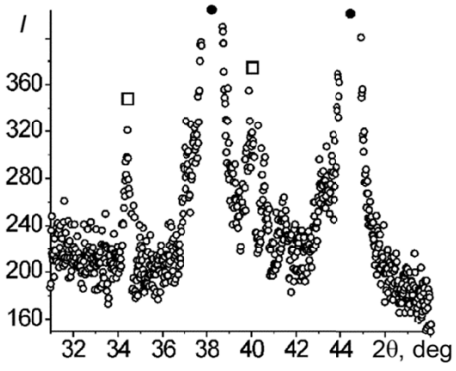

Fig. 3

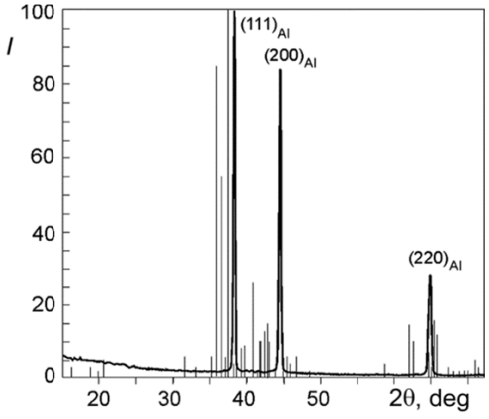

Рис. 4

Fig. 3. Area of the diffraction pattern from the AlMg6 alloy taken in the initial material state (Area *1*, Fig. 1): • – reflections from Al-base solid solution, □ – reflections from the β-Al_2Mg_3-phase.

Рис. 4. Diffraction pattern from the AlMg6 alloy taken from the initial material (Area *1*, Fig. 1) and a line diagram of the β-Al_2Mg_3-phase.

The concentrations of Mg in the solid solution after ultrasonic treatment and in the weld joint zone exceed that in the bulk (even though all the β-Al_2Mg_3-phase particles have been dissolved). In principle, such dissolution could also

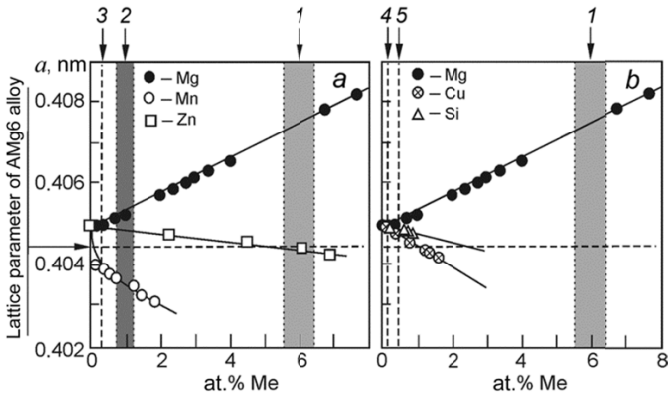

Fig. 5. Lattice parameter variation in solid solutions of Al-alloys as a function of the alloying element concentration. Dotted lines and gray-shaded regions indicate the ranges of the alloying element concentrations: *1* – Mg, *2* – Mn, *3* – Zn, *4* – Cu, *5* – Si. The arrows show the lattice parameter in the initial alloy. The concentration-dependent values of the lattice parameter are taken from [11].

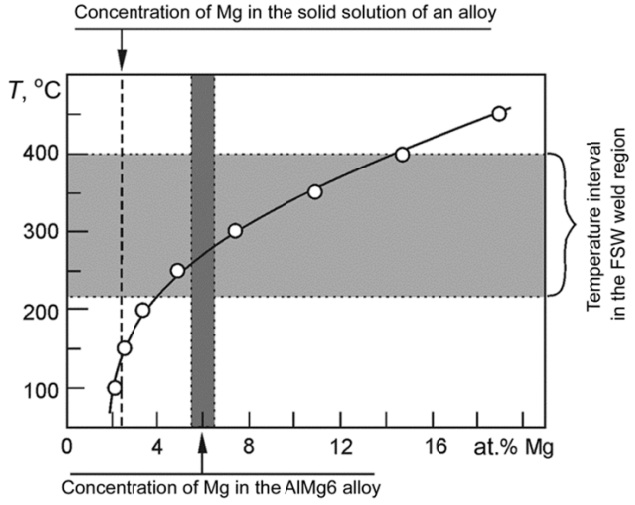

Fig. 6. Solubility of Mg in the FCC-aluminum solid solutions [12].

result from FSW and ultrasonic treatment, since the alloy in the FSW zone is heated to the temperatures within 220–400°C [9]. This is consistent with the data on Mg solubility (Fig. 6). It has to be underlined, however, that even complete dissolution of the β-Al_2Mg_3-particles would not give concentrations higher than 6.5 at.% Mg (see Table 1), thus it does not seem possible to account for the higher values of the lattice parameter of the Al-base solid solution by the dissolution of the β-Al_2Mg_3-phase particles only.

We calculated the first-order stresses generated in the solid solution without taking into account lattice parameter variations due to the changing concentration of Mg atoms in the lattice of the solid solution and found these stresses to be quite high (Table 2).

Thus, the above findings allow us to assume that the lattice parameter values of the alloy solid solution both in the FSW seam and in the ultrasonically treated area are controlled by at least two components: high values of the first-order microstresses and Mg concentration in the solid solution.

TABLE 3. Deformations and Long-Range Second-Order Stresses

Number of area in Fig. 1	Exposure region	CDDs, nm	Strain, %	σII, MPa
1	Initial state	27 ± 1	0.13	254 ± 10
2	Far from the weld with ultrasound	29 ± 1	0.34	664 ± 10
3	Weld zone without ultrasound	40 ± 1	0.06	86.6 ± 10
4	Weld zone with ultrasound	42 ± 1	0.14	184 ± 10

It is to be noted that the calculated stresses are much higher than those far from the weld zone. A subsequent ultrasonic treatment gives rise to a further increase in the lattice parameter and the first-order stresses (hence the long-range stresses also increase), which correlates with increased microhardness (see Table 2). It should be noted that an increase in the long-range stress fields could result in dynamic recrystallization and recovery during friction stir welding.

The calculated values of the second-order stresses and CDD sizes are given in Table 3. Interestingly, the second-order microstresses σ_{II} in the weld zone are lower than those in the initial alloy. This redistribution of stresses could be attributed to the following processes. A decrease in the σ_{II} stresses in the weld zone is associated with their relaxation as a result of stirring after removal of the external impact on the weld joint. It has to be noted that this process occurs under more favorable conditions in the case where the lattice transits into a low-stability state, which is accompanied by considerable structural – phase changes. This correlates with the data reported in [13], where the internal stresses in the grains of severely deformed steel are shown to redistribute as a result of relaxational processes due to a transition grain boundaries from non-equilibrium into equilibrium states. Note also that the deformation impact formed by the field of mechanical stresses during friction stir welding might result in such relaxational processes as the formation of standing waves in a low-stability crystal medium [14].

Thus the X-ray diffractometry data demonstrate that an ultrasonic treatment in the weld zone has resulted in an appreciable increase in the second-order stresses (Table 3).

SUMMARY

The experimental data obtained demonstrate that a combined thermal treatment (weld-zone temperature $T \approx 0.6T_{melt}$) and severe deformation impact on the AlMg6 alloy in the weld joint zone formed by FSW result in a transition of the crystal lattice into a low-stability state. This transition is accompanied by considerable structural-phase transitions manifested as an increased value of the solid-solution lattice parameter in the weld zone. This increase results both from high internal stresses and increased concentrations of Mg atoms in the solid solution due to essential dissolution of the β-Al_2Mg_3-phase particles with a higher content of manganese than that in the base material. The above-mentioned processes are accompanied by high-intensity diffusion and relaxation due to the low-stability state of the crystal lattice (inhomogeneous stresses) in the weld joint zone. These phenomena favor mixing of the atoms in the alloy during friction stir welding.

REFERENCES

1. M. Jayraman and V. Balasubramanian, Trans. Nonferrous Met. Soc. China, No. 23, 605–615 (2013).
2. S. Mironov, Y.S. Sato, H. Kokawa. Acta Materialia. **57**, P. 4519–4528 (2009).
3. A. A. Klopotov, Yu. A. Abzaev, A. I. Potekaev, and O. G. Volokitin, Fundamentals of X-Ray Structural Analysis in Materials Science [in Russian], Tomsk, TGASU Publ. (2012).
4. E. A. Kolubaev, Russ. Phys. J., **57**, No. 10, 1321–1327 (2015).
5. Qifang Zhu, Zeming Sun, Tongda Ma, *et al*., Mater. Sci. Forum, **654–656,** 1892–1895 (2010).

6. A. I. Potekaev, A. A. Klopotov, E. V. Kozlov, and V. V. Kulagina, Low-Stability Pretransitional Structures in Nickel Titanium [in Russian], Tomsk, NTL Publ. (2004).
7. A. I. Potekaev, A. A. Klopotov, M. M. Morozov, *et al*., Structural Features of Binary Systems with Low-Stability States [in Russian], Tomsk, NTL Publ. (2014).
8. A. M. Glazer, A. I. Potekaev, and A. O. Cheretaeva, Time-Temperature Stability of Amorphous Alloys [in Russian], Tomsk, NTL Publ. (2015).
9. A. A. Khaidarova, V. A. Klimenov, A. V. Azarkin, *et al*., Zh. Kontrol. Diagnostika, No. 13, 186–191 (2013).
10. A. P. Babichev, N. A. Babushkina, *et al*., Physical Quantities: a reference book [in Russian], Moscow, Energoatomizdat (1991).
11. W. B. Pearson, A Handbook of Lattice Spacing and Structures of Metals and Alloy, London – New York, Pergamon Press (1958).
12. N. P. Lakisheva, State Diagrams of Binary Metal Systems [in Russian], Moscow, Mashinostroyeniye (1996).
13. S. V. Makarov, V. A. Plotnikov, and A. I. Potekaev, Russ. Phys. J., **57**, No. 4, 436–440 (2014).
14. S. V. Makarov, V. A. Plotnikov, A. I. Potekaev, and L. S. Grinkevich, Russ. Phys. J., **57**, No. 12, 1676–1682 (2015).